Estimation of borehole ellipticity using cross-dipole dispersions

Ergun Simsek and Bikash K. Sinha, Schlumberger-Doll Research

Summary

The presence of a large differential stress in the borehole cross-sectional plane can cause a circular borehole to deform into an elliptical cross-section. If the borehole fluid pressure is below a safe threshold, a compressive shear failure of rock causes symmetric borehole breakouts. Both borehole ellipticity and breakouts cause flexural wave splitting in the intermediate frequency band where the flexural wavelength is comparable to the borehole diameter. This paper describes a technique for estimating the borehole ellipticity using the even and odd flexural dispersions. For both forward and inverse solvers, a boundary-integral method is used to generate even and odd flexural dispersions for an elliptical borehole cross-section. The underlying theory is based on sensitivity analyses of measured even and odd flexural dispersions to changes in the borehole ellipticity. The proposed technique has been validated using synthetic examples of borehole dispersions in the presence of elliptical boreholes.

Introduction

The presence of a fluid-filled borehole in a prestressed formation causes near-wellbore stress concentrations. A vertical borehole with a circular cross-section can deform into an elliptical borehole in compliant formations subject to the far-field horizontal stresses. While the borehole fluid pressure is designed to maintain static equilibrium with the surrounding formation, there are instances when the compressive hoop stress at the borehole surface exceeds the rock yield stress resulting in elliptical boreholes or borehole breakouts. Generally, breakouts occur during underbalance drilling or surge and swab operation performed by drillers. The major axis of an elliptical borehole and breakout azimuth coincide with the minimum horizontal stress direction and the distorted borehole cross-section can be used to estimate the maximum horizontal stress magnitude (Bell and Gough, 1983; Zoback et al., 1985; Vernik and Zoback, 1992; Grandi and Toksöz, 2005). A detailed borehole cross-sectional image is obtained by a four-arm dipmeter and an ultrasonic imaging tool that operates in a pulse-echo mode (Plumb and Hickman, 1985).

Borehole cross-section affects the propagation of guided modes, such as the lowest-order axi-symmetric Stoneley, flexural, and quadrupole modes. In a previous paper, Simsek et al. (2007) presented a study of the influence of borehole breakouts on the Stoneley, flexural, and quadrupole modes using the FDTD method with a PML to minimize reflections from the outer boundary. They also confirmed that flexural waves split in the intermediate frequency band where the flexural wavelength is comparable to the borehole diameter. Since changes in borehole cross-section can be identified by monitoring perturbations in the guided mode dispersions from a reference circular borehole case, Simsek and Sinha (2007) developed a perturbation model to analyze non-circular boreholes. In that work, they validated their perturbation model by comparing with a boundary-integral equation (BIE) method. One of the results of these previous studies is that for a fast formation, even modes and for a slow formation, odd modes are more sensitive to changes in the borehole elongation. Based on this observation, here we develop an efficient and robust algorithm to estimate major and minor radii of an elliptical borehole in fast formations using cross-dipole dispersions.

In this work, we continue to use BIE method (Randall, 1991) to invert measured borehole flexural dispersions. While non-symmetric distortion of boreholes are also known to occur, we plan to analyze in this paper elliptical boreholes that lead to splitting of flexural waves into two canonical waves. We use a fast mode search algorithm to obtain monopole and dipole dispersions of a fluid-filled circular borehole where the solution is obtained by satisfying appropriate boundary condition at the liquid-solid boundary (Sinha and Asvadurov, 2004).

Theory

Figure 1 shows a schematic diagram of a fluid-filled elliptical borehole. r_{major} and r_{minor} are the two principal radii of the ellipse. In the field, a single caliper might measure either of these values or something between them. The aim of this work is to obtain r_{major} and r_{minor} values accurately for an arbitrary caliper reading, $r_{caliper}$ ($r_{minor} \le r_{caliper} \le r_{major}$) using the even and odd flexural dispersions.

We use a mode search algorithm to obtain flexural dispersions for a circular borehole and a BIE method for non-circular boreholes. In BIE, displacement and stresses on the borehole wall are described by integrals over a surface distribution of effective sources, in the frequency-axial wave number ($\omega - k_z$) domain. The unknown sources are approximated by sums of finite basis functions, which are then determined by enforcing boundary conditions. The discretized equations form a homogeneous system whose determinant vanishes when ($\omega - k_z$) correspond to a nontrivial solution for the mode of interest.

We assume that the physical properties (mass density, compressional and shear velocities) of formation and borehole liquid are known. The slowness dispersions for an even (S_e, f_e), and odd (S_o, f_o) modes of an elliptical borehole, and $r_{caliper}$ are assumed to be known. Here we use

the notation that S and f denote slowness (inverse of velocity) and frequency, respectively. N_e and N_o denote the number of data samples for even and odd modes, respectively.

We first calculate the flexural dispersion, (S_c, f_c), for a circular borehole of radius $r_{caliper}$, together with formation and fluid properties. We know that (S_c, f_c) forms a discrete function: $F(S_c)= f_c$. We need to construct new data points (frequencies) from S_e and S_o, separately, to find corresponding frequencies of the circular case to these slownesses, such that $F(S_e)= f_{e,0}$ and $F(S_o)= f_{o,0}$. To do that, we use a cubic spline interpolator (CSIEZ, from IMSL® numeric library). Averages of the interpolation results normalized by f_e for even, and f_o for (odd) mode yield regularization parameters α_0 and β_0 for a fast formation. However, since ellipticity has opposite effects in slow formations, we need to interpolate and average odd modes to obtain α_0, and average even modes to obtain β_0.

The second step is the iterative part of the algorithm. At j^{th} step, we use BIE to generate flexural dispersions for an elliptical borehole with radii of $r_{major,j}$ and $r_{minor,j}$, where $r_{major,j}=\alpha_{j-1} \times r_{major,j-1}$ and $r_{minor,j}=\beta_{j-1} \times r_{minor,j-1}$. Note that for the first iteration $r_{major,0}= r_{minor,0}=r_{caliper}$. Then we again use an interpolator to find the corresponding f_c values for the given S_e and S_o, separately. New averages give us new regularization parameters α_j and β_j. As we iterate more, α_j and β_j both approach 1. Once the error criterion is satisfied, we can quit the "while loop". We can formulate this algorithm as follows:

Calculate circular borehole's flexural dispersion: (S_c, f_c)
Interpolate(S_c, f_c, S_e) = $f_{e,0}$
Interpolate(S_c, f_c, S_o) = $f_{o,0}$
$r_{major,0} = r_{minor,0} = r_{caliper}$
i=0
if "a fast formation"

$$\alpha_i = \frac{1}{N_e}\sum_{n=1}^{N_e}\frac{f_{e,i}}{f_e}, \qquad \beta_i = \frac{1}{N_o}\sum_{n=1}^{N_o}\frac{f_{o,i}}{f_o} \qquad (1)$$

else

$$\alpha_i = \frac{1}{N_o}\sum_{n=1}^{N_o}\frac{f_{o,i}}{f_o}, \qquad \beta_i = \frac{1}{N_e}\sum_{n=1}^{N_e}\frac{f_{e,i}}{f_e} \qquad (2)$$

end if
while $|\alpha_i\text{-}1|>\varepsilon_{tol}$ *and* $|\beta_i\text{-}1|>\varepsilon_{tol}$
j=i+1
$r_{major,j} = \alpha_i \times r_{major,i}$ and $r_{minor,j} = \beta_i \times r_{minor,i}$
Use BIE for the elliptical case with ($r_{major,j}$, $r_{minor,j}$) *and obtain* (S_e', f_e') *and* (S_o', f_o')
Interpolate(S_e', f_e', S_e) = $f_{e,j}$
Interpolate(S_o', f_o', S_o) = $f_{o,j}$
Calculate α_j *and* β_j *using either Eq. (1) or (2) depending on formation shear*
i=i+1
end.

To speed up the BIE solution, mode-search results can be used to narrow the (ω–k_z) search region. In this case, mode search results should be updated for a circular borehole with a radius of $r_{minor,i}$ at each step for the lower boundary. For a slow formation, monopole dispersion can be used as an upper boundary as well.

The overall method can be seen as a Newton's method (Tjalling, 1995), where the initial guess is a circular case with a radius of $r_{caliper}$, which guarantees a reasonably good guess.

Computational results in a fast formation

The formation compressional and shear velocities are 4848 and 2601 m/s, respectively, whereas the mass density is 2160 kg/m^3. The borehole fluid compressional velocity is 1500 m/s, and its mass density is 1000 kg/m^3. The minor and major radii of elliptical borehole are 10 and 11 cm, respectively. Assume that even and odd flexural dispersions are given, see Figure 2, and the radius of the borehole measured by a caliper is 10.5 cm.

We first calculate the flexural dispersion of a circular borehole with a radius of 10.5 cm for a given formation and fluid properties using a mode-search algorithm. Then we calculate first regularization parameters as described above, which results in 10.7868 and 9.87369 cm for r_{major} and r_{minor}, respectively. Even at the end of first step, the overall error is less 2 %. Then iterative part of the algorithm starts. We set the error tolerance to 0.0005 (0.05 %). Table 1 shows convergence of r_{major} and r_{minor} to the actual values of elliptical borehole's radii as a function of iteration. Notice that the regularization parameters α_i and β_i converge to 1 as expected. As it can be seen from Table 1 and Figure 3, we satisfy our error tolerance at the end of 5 iterations. The final estimated values for r_{major} and r_{minor} are 10.9994 and 10.00002 cm. Figure 2 shows the comparison of input dispersions and the ones obtained using these final estimates.

Iteration Number	r_{minor}	β_i	r_{major}	α_i
0 (Initial)	10.5	-	10.5	-
1	9.87369	0.9404	10.7868	1.0273
2	10.06936	1.0198	10.9879	1.0186
3	9.99500	0.9926	10.9919	1.0004
4	9.99966	1.0005	10.9982	1.0006
5	10.00002	1.0000	10.9994	1.0001

Table 1. Convergence of the algorithm for a fast formation.

In this example, the frequency range (bandwidth) of the data is between 3 and 10 kHz. Higher end of this bandwidth has smaller wavelength which means a better resolution. As a result, the high frequency part of the input data gives us more information about borehole elongations.

However, the measured field data might have a significantly shorter bandwidth. To study this situation, we generate another set of input data, which has 3 kHz bandwidth, from 4 to 7 kHz. Table 2 follows the notation presented in Table 1. In this case, we can meet our error criterion after 6 iterations, which clearly indicates the robustness and efficiency of the algorithm.

Iteration Number	r_{minor}	β_i	r_{major}	α_i
0 (Initial)	10.5	-	10.5	-
1	9.93844	0.9465	10.7981	1.0284
2	13.0645	1.3145	11.967	1.1083
3	10.11596	0.7743	10.8797	0.9091
4	9.99557	0.9881	10.966	1.0079
5	9.9998	1.0004	10.9941	1.0026
6	10.00001	1.00001	10.999	1.0004

Table 2. Convergence of the algorithm for a fast formation using dispersions with a limited bandwidth.

Computational results in a slow formation

We follow the same procedure for a slow formation that has a mass density of 2000 kg/m^3 and 2545 and 1018 m/s for compressional and shear velocities, respectively. The borehole fluid is same as previous case. The minor and major radii of elliptical borehole are 10 and 13 cm, respectively. Assume that even and odd flexural dispersions are given, see Figure 4, and the radius of the borehole measured by a caliper is 11 cm.

Table 2 shows convergence of r_{major} and r_{minor} to the actual values of elliptical borehole's radii as a function of iteration for the slow formation. Again, regularization parameters α_i and β_i converge to 1 as expected. As it can been seen from Table 2 and Figure 5, it takes only 6 iterations to meet our error criterion (0.05 %) and Figure 4 shows accuracy of the estimation by comparing the input dispersions and the ones obtained using the 6th iteration's estimates.

Iteration Number	r_{minor}	β_i	r_{major}	α_i
0 (Initial)	11.0	-	11.0	-
1	9.90123	0.90012	11.9291	1.0845
2	10.12157	1.02225	12.9366	1.0845
3	10.03020	0.99097	12.9754	1.0030
4	10.00863	0.99784	12.9918	1.0013
5	10.00315	0.99945	12.9963	1.0003
6	10.00023	0.99970	12.9970	1.0001

Table 3. Convergence of the algorithm for a slow formation.

In this example, we have used flexural dispersions with a bandwidth from 1 to 6 kHz. To study the influence of a shorter bandwidth, we show estimates of the major and minor radii of the ellipse using a bandwidth from 1.5 to 4 kHz. Table 4 shows that convergence to the final values is obtained after 10 iterations.

Iteration Number	r_{minor}	β_i	r_{major}	α_i
0 (Initial)	11	-	11	-
1	10.20866	0.9281	11.8859	1.0805
2	10.21767	1.0009	12.6827	1.0670
3	10.10117	0.9886	12.8703	1.0148
4	10.04525	0.9945	12.9448	1.0058
5	10.01907	0.9974	12.9748	1.0023
6	10.00769	0.9989	12.9875	1.0010
7	10.00327	0.9996	12.9924	1.0004
8	10.00198	0.9999	12.9945	1.0002
9	10.00087	0.9999	12.9959	1.0001
10	10.00064	1.0000	12.9986	1.0002

Table 4. Convergence of the algorithm for a slow formation using dispersions with a limited bandwidth.

Summary and Conclusions

We have developed an inversion algorithm to estimate major and minor radii of a fluid-filled elliptical borehole using cross-dipole dispersions. Starting from a reference circular fluid-filled borehole with an arbitrary radius measured by a single-arm caliper, this algorithm minimizes differences between measured even and odd flexural dispersions, and that for the reference circular borehole to obtain the major and minor radii of an elliptical borehole. In fast formations, we use even and odd dispersions with an interpolator to calculate the regularization parameter giving r_{major} and r_{minor}, respectively. In contrast, we use odd and even dispersions in slow formations with an interpolator to calculate the regularization parameter giving r_{major} and r_{minor}, respectively. Numerical results show that accurate results (relative error < 1 %) can be obtained after a small number of iterations even for flexural dispersions with a limited bandwidth.

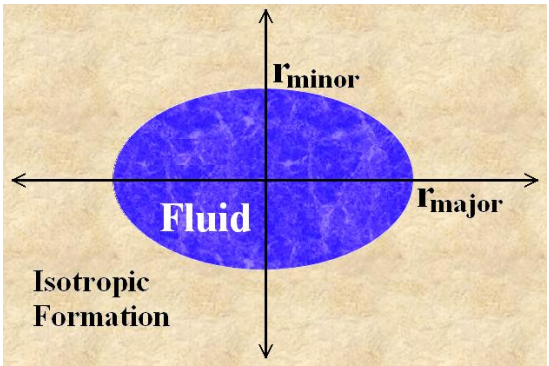

Figure 1. Schematic of an elliptical fluid-filled borehole cross-section surrounded by a formation.

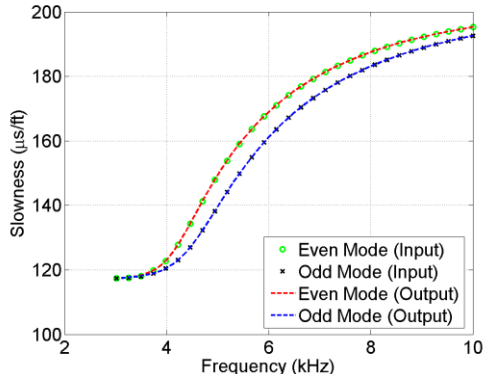

Figure 2. Green circle and black cross markers show synthetically generated even and odd flexural dispersions, respectively, for an elliptical borehole (10 cm, 11 cm) surrounded by a fast formation. The dashed red and blue lines depict reconstructed dispersions for even and odd modes, respectively, after the major and minor radii have been estimated.

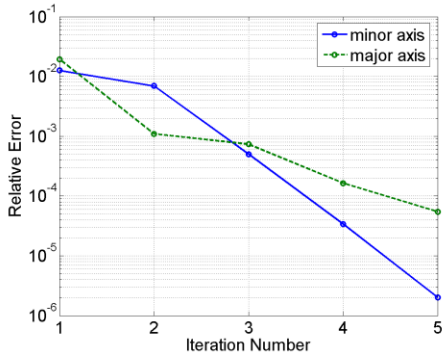

Figure 3. Blue solid and green dashed lines show the relative error for minor and major radii, respectively, as a function of iteration number. The result depicted in Figure 2 is obtained using r_{minor} and r_{major} values after 6 iterations (Bandwidth 3 to 10 kHz).

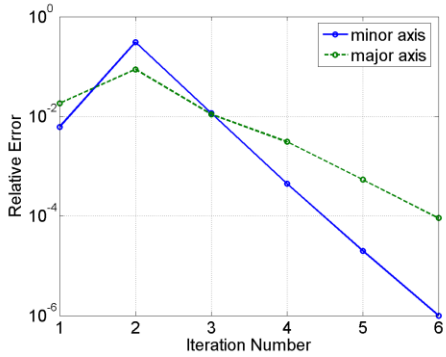

Figure 4. Blue solid and green dashed lines show the relative error for minor and major radii, respectively, as a function of iteration number (Bandwidth 4 to 7 kHz).

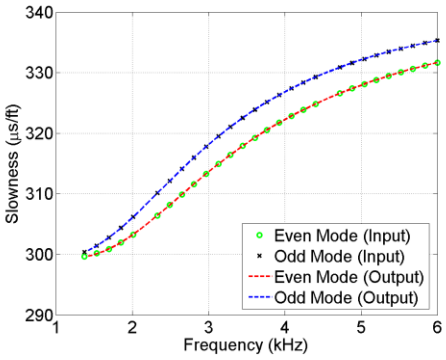

Figure 5. Green circle and black cross markers show synthetically generated even and odd flexural dispersions, respectively, for an elliptical borehole (10 cm, 13 cm) surrounded by a slow formation. The dashed red and blue lines depict reconstructed dispersions for even and odd modes, respectively, after the major and minor radii have been estimated.

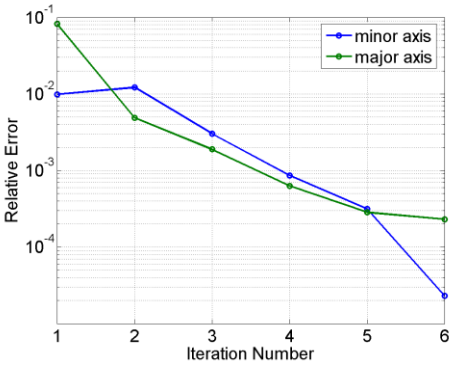

Figure 6. Blue solid and green dashed lines show the relative error for minor and major radii, respectively, as a function of iteration number. The result depicted in Figure 4 is obtained using r_{minor} and r_{major} values from the 6th iteration (Bandwidth 1 to 6 kHz).

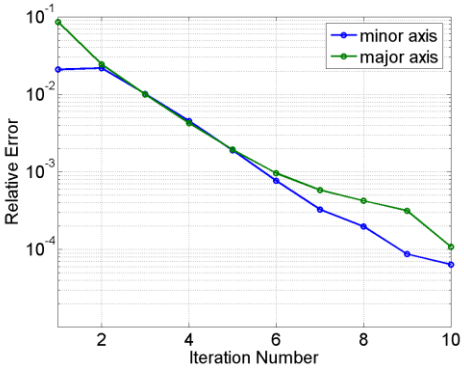

Figure 7. Blue solid and green dashed lines show the relative error for minor and major radii, respectively, as a function of iteration number (Bandwidth 1.5 to 4 kHz).

EDITED REFERENCES

Note: This reference list is a copy-edited version of the reference list submitted by the author. Reference lists for the 2008 SEG Technical Program Expanded Abstracts have been copy edited so that references provided with the online metadata for each paper will achieve a high degree of linking to cited sources that appear on the Web.

REFERENCES

Bell, J. S., and D. I. Gough, 1983, The use of borehole breakout in the study of crustal stress, *in* M. D. Zoback and B. C. Haimson, eds., Hydraulic fracturing stress measurements: National Academic Press, 201–209.

Grandi, S., and N. Toksöz, 2005, In situ stress field from borehole measurements and plate tectonic models: AGU Spring Meeting Abstracts, May.

Plumb, R. A., and S. H. Hickman, 1985, Stress-induced borehole elongation: A comparison between the four-arm dipmeter and the borehole televiewer in the Auburn geothermal well: Journal of Geophysical Research, **90**, 5513–5522.

Randall, C. J., 1991, Modes of noncircular fluid-filled boreholes in elastic formations: Journal of the Acoustical Society of America, **89**, 1002–1016.

Sinha, B. K., and S. Asvadurov, 2004, Dispersion and radial depth of investigation of borehole modes: Geophysical Prospecting, **52**, 271–286.

Simsek, E., and B. K. Sinha, 2007, Analysis of noncircular fluid-filled boreholes in elastic formations using a perturbation model, submitted for publication.

Simsek, E., B. K. Sinha, S. Zeroug, and N. Bounoua, 2007, Influence of breakouts on borehole dispersions: Presented at the 77th Annual International Meeting, SEG.

Vernik, L., and M. D. Zoback, 1992, Estimation of maximum horizontal principal stress magnitude from stress-induced wellbore breakouts in the Cajon Pass Scientific Research Borehole: Journal of Geophysical Research, **97**, 5109–5119.

Tjalling, J. Y., 1995, Historical development of the Newton-Raphson method, SIAM Review, **37**, 531–551.

Zoback, M. D., D. Moos, L. Mastin, and R. N. Anderson, 1985, Wellbore breakouts and in-situ stress: Journal of Geophysical Research, **90**, 5523–5530.